Routes for Rapid Synthesis of Photovoltaic Absorber Materials: The Need for Diffusion Data

Ranga Krishnan, Gabriel Tong, Chris Muzzillo, Woo Kyoung Kim, Tim Anderson (UF), Andrew Payzant (ORNL), Carelyn Campbell, Ursala Kattner (NIST), and Jianyun Shen (Beijing Inst. Met.)

Jevons Paradox

Technological progress that increases the efficiency with which a resource is used, tends to increase (rather than decrease) the rate of consumption of that resource.

William Stanley Jevons

Simple Diode

Analysis for a 24%-efficient Si solar cell

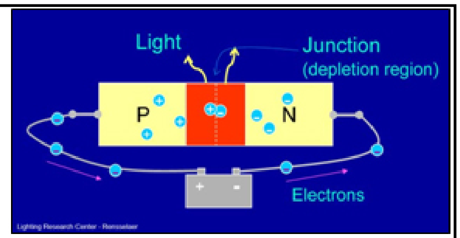

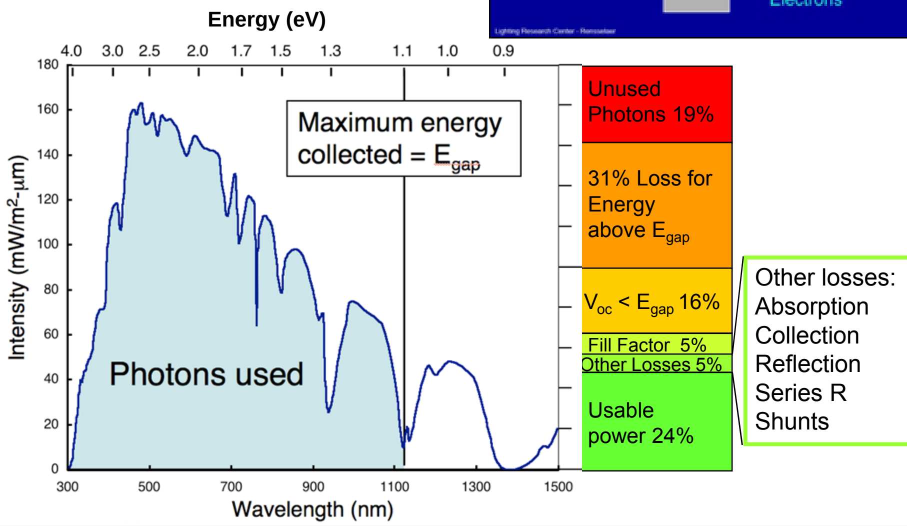

Photovoltaic Technologies

- **First generation**
  - Single crystal and multicrystalline Si
  - a-Si:H single junctions
- **Second generation**
  - Inorganic thin films ($CuInSe_2$ & CdTe)
  - Multijunction III-V & a-Si:H
- **Third generation**
  - Nanostructured & quantum dot PV
  - Photoelectrochemical cells
  - Organic photovoltaics
  - Intermediate band concepts

(PV-Tech.org)

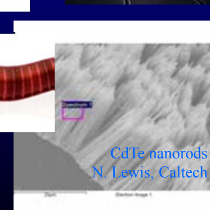

Routes to Increased Efficiency

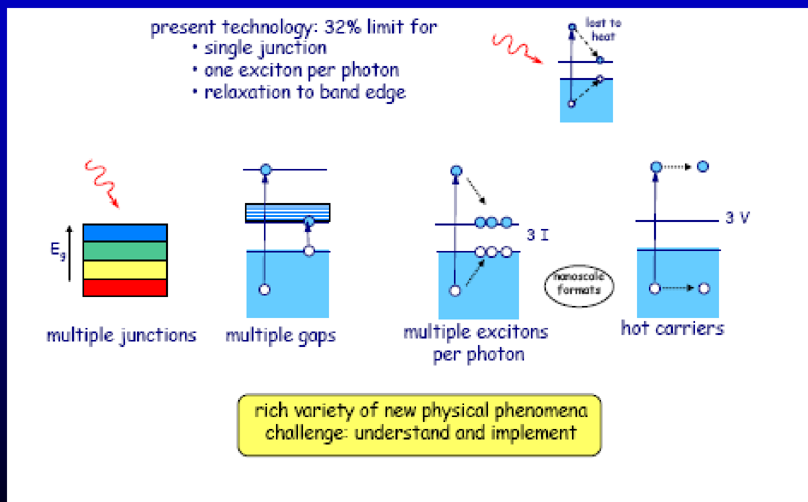

www1.eere.energy.gov/solar/solar_america/pdfs/d_horwitz_os_bes.pdf

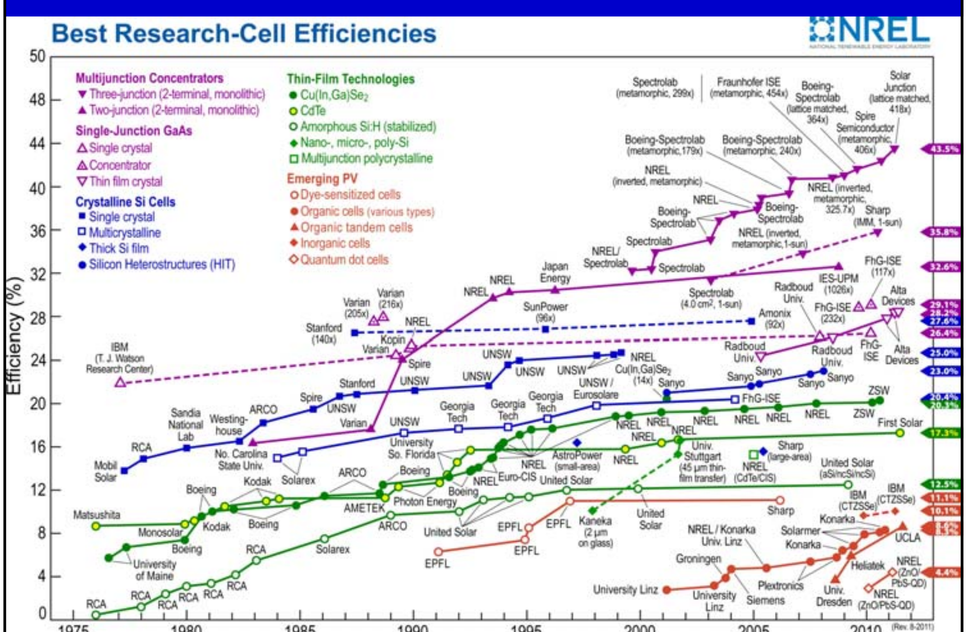

$Cu(In_{1-x}Ga_x)Se_2$ Solar Cells

Most Promising Thin Film Absorber Material

- Direct band gap (Eg ~ 1.2 eV)
- High optical absorption coefficient: ~ 2 µm
- High radiation resistance
- High reliability
- Lower cost per Watt installed
- High conversion efficiency: cell: 20% and module: 13%
- Efficient in low-angle & low-light conditions
- Flexible substrates possible (BIPV, cheaper substrates?)
- Positive response under concentration

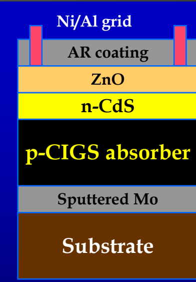

CIGS solar cell structure

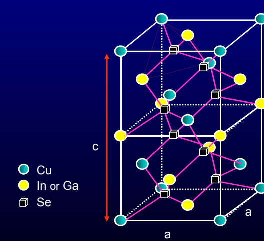

Chalcopyrite structure

NREL 3-stage Process: Champion Cell

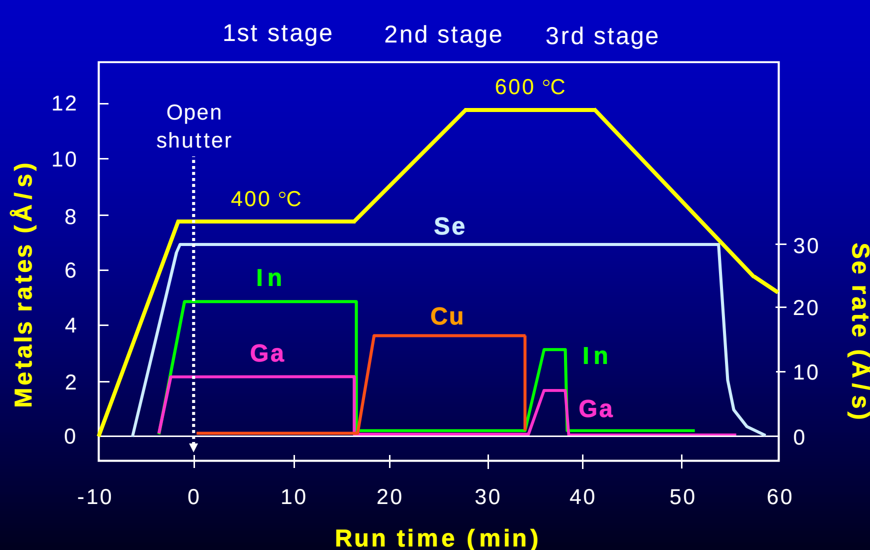

Approaches to CIGS Synthesis

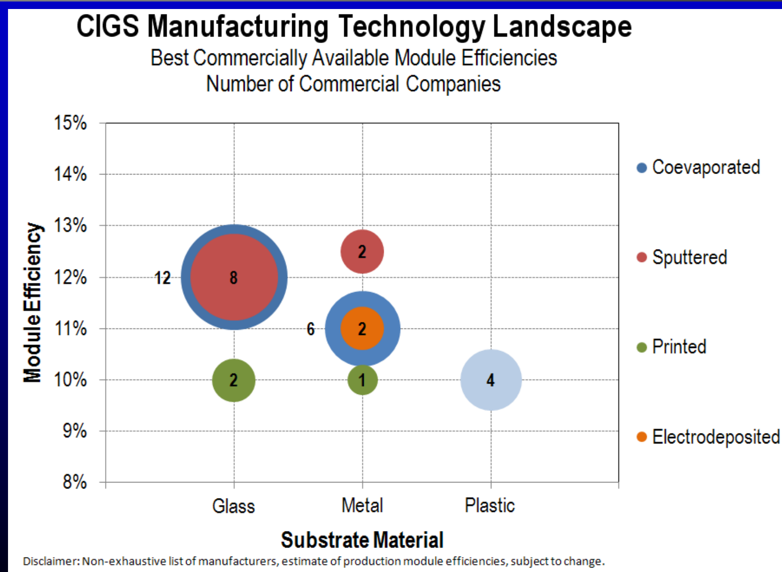

CIGS Manufacturing Costs

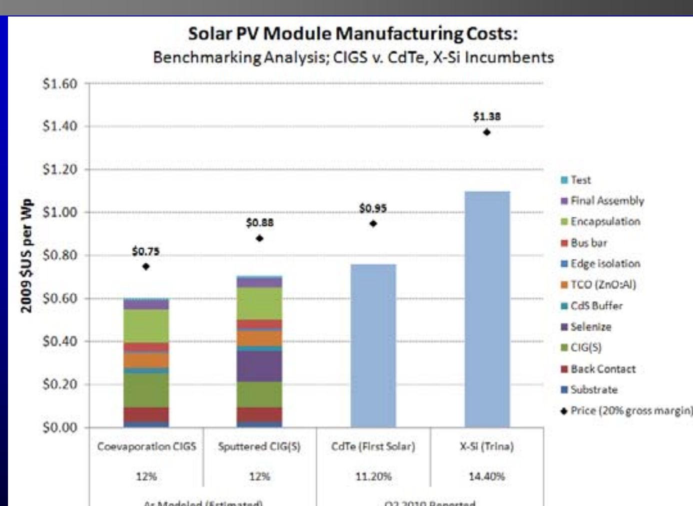

Module costs must be considered in the context of module efficiency (impact on installation costs)

Courtesy of NREL

The Value Proposition for High Efficiency CIGS

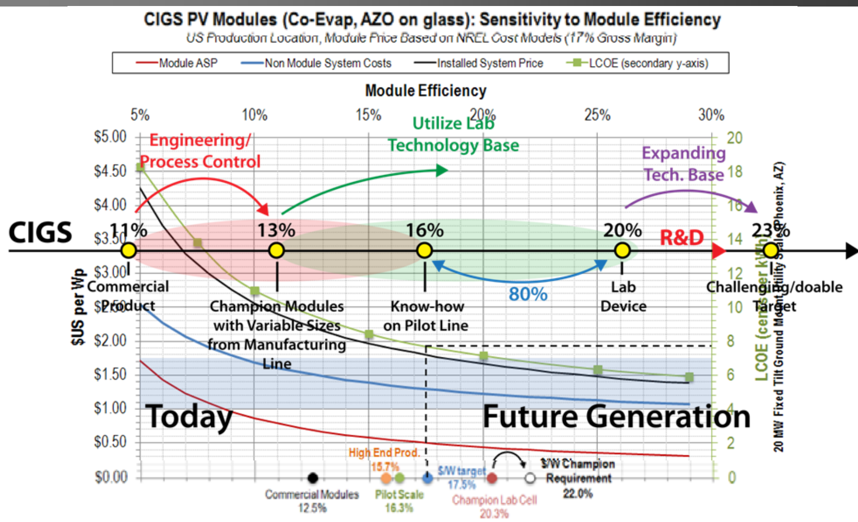

- At no added cost ($\$/m^2$), 17.5% CIGS module = ~$0.50/Wp module ASP target
- New champion lab cell efficiency (≥22%), BoS improvements are required

Courtesy of NREL

Future Challenges and Opportunities

Device structure varies between monolithically & mechanically integrated modules

Today	Front Contact Grid	Forward
	• Screen Print Ag	• Reduce shadowing • Faster application
ZnO, ITO (2500 Å) • Sputter		Hardened TCO (moisture barrier)
CdS (700 Å) • Chemical Bath Deposition • Sputter		Cd-free; dry, eliminate
CIGS (1-2.5 µm) • Multiple methods (coevaporation, sputtering, printing, electrodeposition)		Increase Ga-%, Reduce thickness, Rapid deposition Uniformity (composition, temp., thickness)
Mo (0.5-1 µm) • Sputter		Na dosing
Glass, Metal Foil, Plastics		High temp. glass Metal foils: smooth, flex-dielectric (monolith.)

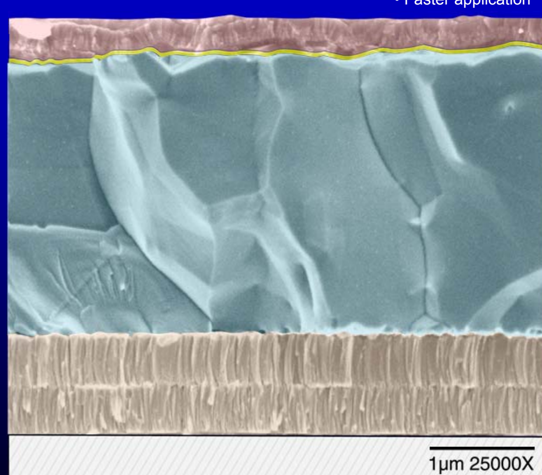

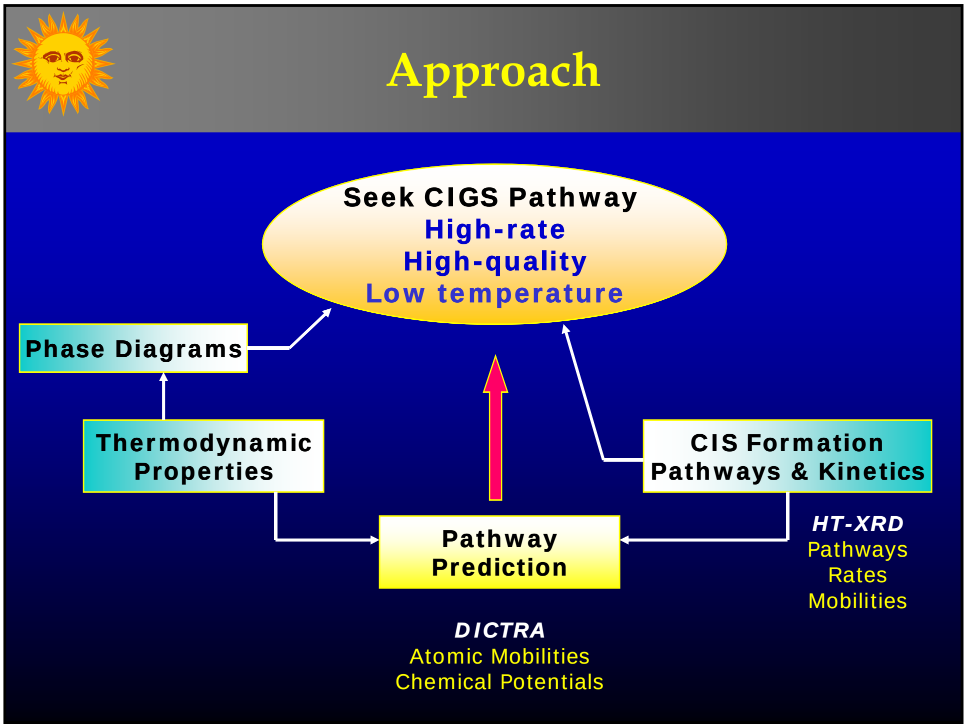
Approach
Seek CIGS Pathway
High-rate
High-quality
Low temperature
Phase Diagrams
Thermodynamic Properties
CIS Formation Pathways & Kinetics
Pathway Prediction
HT-XRD
Pathways
Rates
Mobilities
DICTRA
Atomic Mobilities
Chemical Potentials

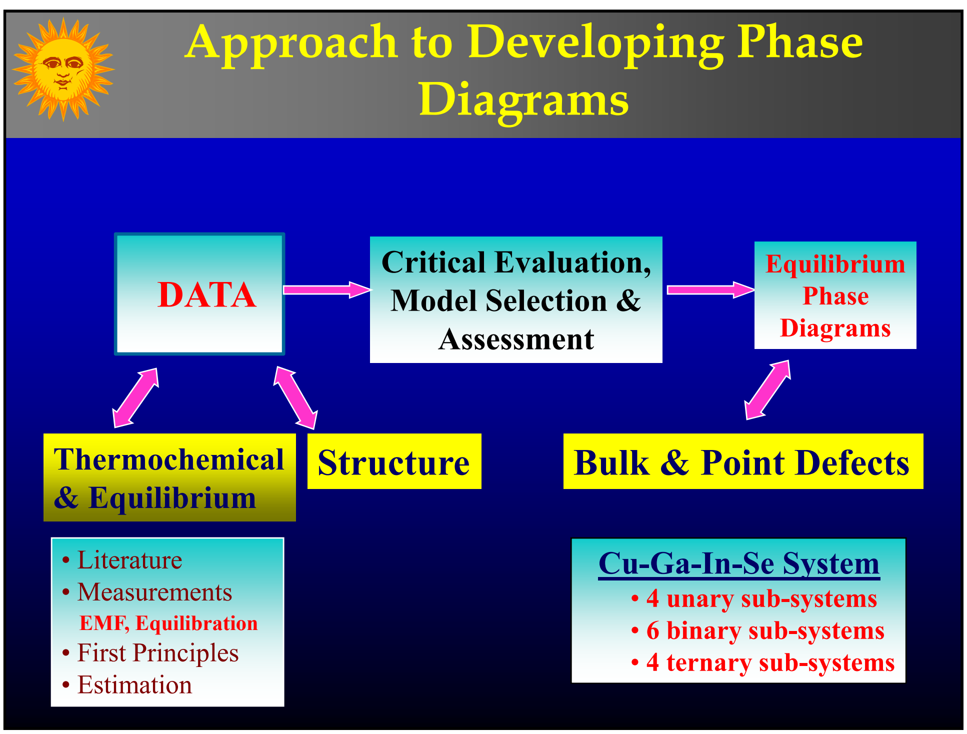
Approach to Developing Phase Diagrams
DATA
Critical Evaluation, Model Selection & Assessment
Equilibrium Phase Diagrams
Thermochemical & Equilibrium
Structure
Bulk & Point Defects
• Literature
• Measurements
EMF, Equilibration
• First Principles
• Estimation
Cu-Ga-In-Se System
• 4 unary sub-systems
• 6 binary sub-systems
• 4 ternary sub-systems

Comparison of Calculated Cu-Se Phase Diagram with Experimental Data

Phase	Model
Liquid	Ionic two sub-lattice model (Cu+1,Cu+2)p(Se-2,Va,Se)q
α-$Cu_{2-x}Se$	Sub-lattice model (3 sub-lattices) $(Cu,Va)_1(Se,Va)_1(Cu)_1$
β-$Cu_{2-x}Se$	Sub-lattice model (3 sub-lattices) $(Cu,Va)_1(Se,Va)_1(Cu)_1$
Fcc (Cu)	Regular solution model

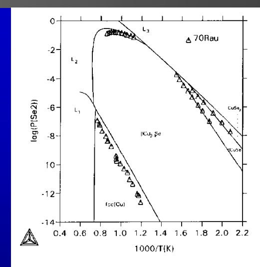

Se_2 Partial Pressure

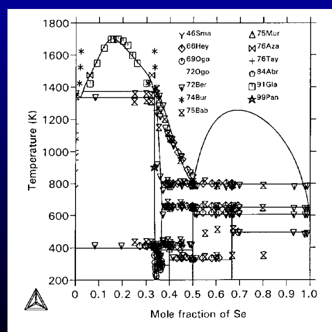

W/Cu,Cu_2O//YSZ//$Cu_{2-x}Se$, Cu_2O/C/W

[Cu] ↔ $Cu_{[Cu_{2-x}Se]}$ ln a_{Cu} = -FE/RT

V_{Cu} in $Cu_{2-x}Se$

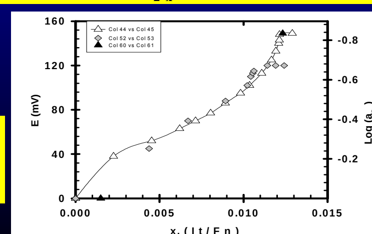

Phase Equilibria in Cu-In-Ga-Se System

Cu-In-Ga-Se

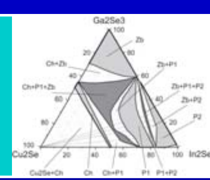

Cu-In-Ga

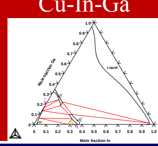

Cu-In-Se

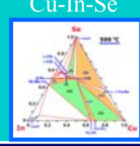

Cu_2Se-Ga_2Se_3

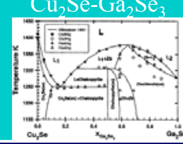

Cu_2Se-In_2Se_3

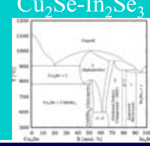

Cu-In

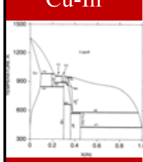

Cu-Ga

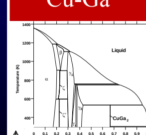

In-Ga

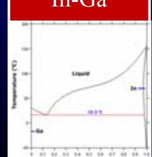

Cu-Se

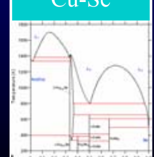

In-Se

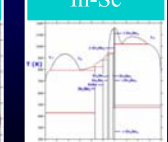

Ga-Se

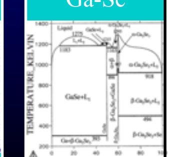

Phase Diagram of Cu-In-Se

Isothermal section at 500 °C
(18 phases)

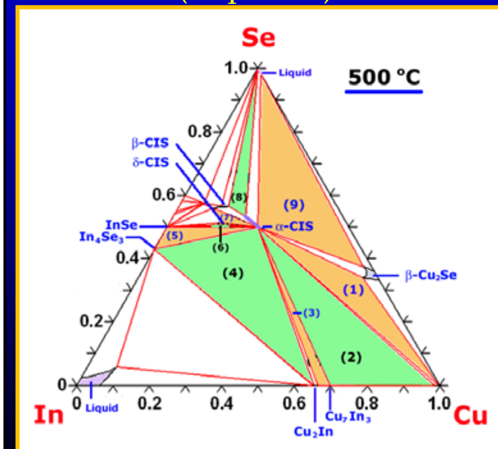

Region	Equilibrium phases
1	α-$CISe_2$ + α-Cu + β-Cu_2Se
2	α-$CISe_2$ + α-Cu + Cu_7In_3
3	α-$CISe_2$ + Cu2In + Cu_7In_3
4	α-$CISe_2$ + Cu2In + In_4Se_3
5	α-$CISe_2$ + InSe + In_4Se_3
6	α-$CISe_2$ + InSe + δ-$CuInSe_2$
7	α-$CISe_2$ + β-$CuIn_3Se_5$ + δ-$CuInSe_2$
8	α-$CISe_2$ + β-$CuIn_3Se_5$ + Liquid
9	α-$CISe_2$ + β-Cu_2Se + Liquid

Chemical Potential Diagram

Wide molecularity range yields 18 to >20% devices
Cu/(In+Ga): 0.95 to 0.82 and Ga/(In+Ga): 0.26 to 0.35

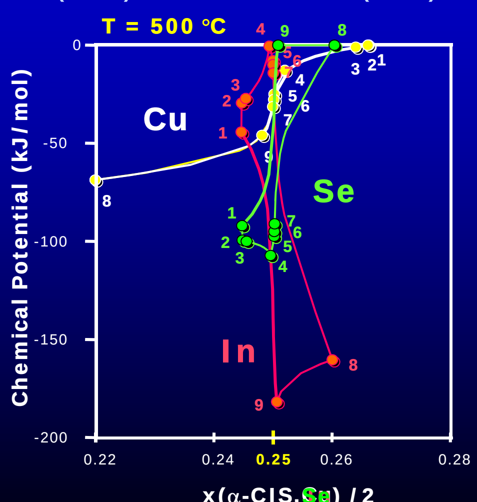

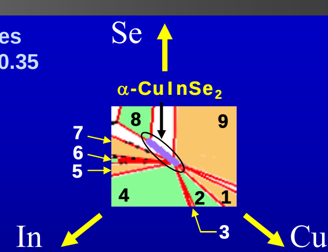

Reg.	Equilibrium phases
1	α-$CISe_2$ + α-Cu + β-Cu_2Se
2	α-$CISe_2$ + α-Cu + Cu_7In_3
3	α-$CISe_2$ + Cu_2In + Cu_7In_3
4	α-$CISe_2$ + Cu_2In + In_4Se_3
5	α-$CISe_2$ + InSe + In_4Se_3
6	α-$CISe_2$ + InSe + δ-$CuInSe_2$
7	α-$CISe_2$ + β-$CuIn_3Se_5$ + δ-$CuInSe_2$
8	α-$CISe_2$ + β-$CuIn_3Se_5$ + Liquid
9	α-$CISe_2$ + β-Cu_2Se + Liquid

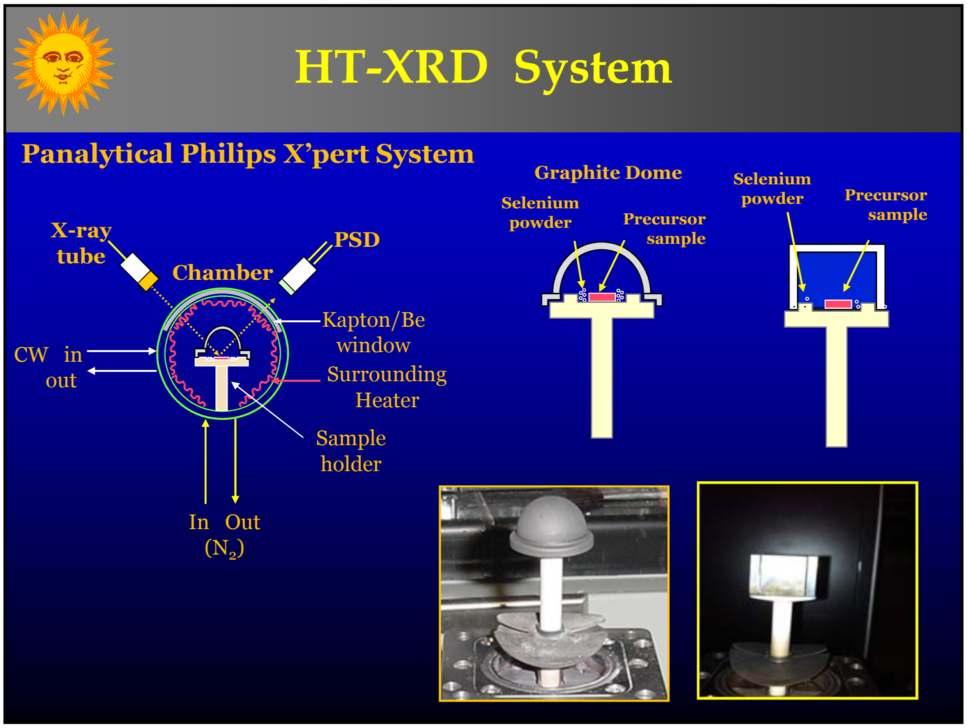
HT-XRD System
Panalytical Philips X'pert System
X-ray tube
PSD
Chamber
Kapton/Be window
CW in
out
Surrounding Heater
Sample holder
In Out
(N2)
Graphite Dome
Selenium powder
Precursor sample
Selenium powder
Precursor sample

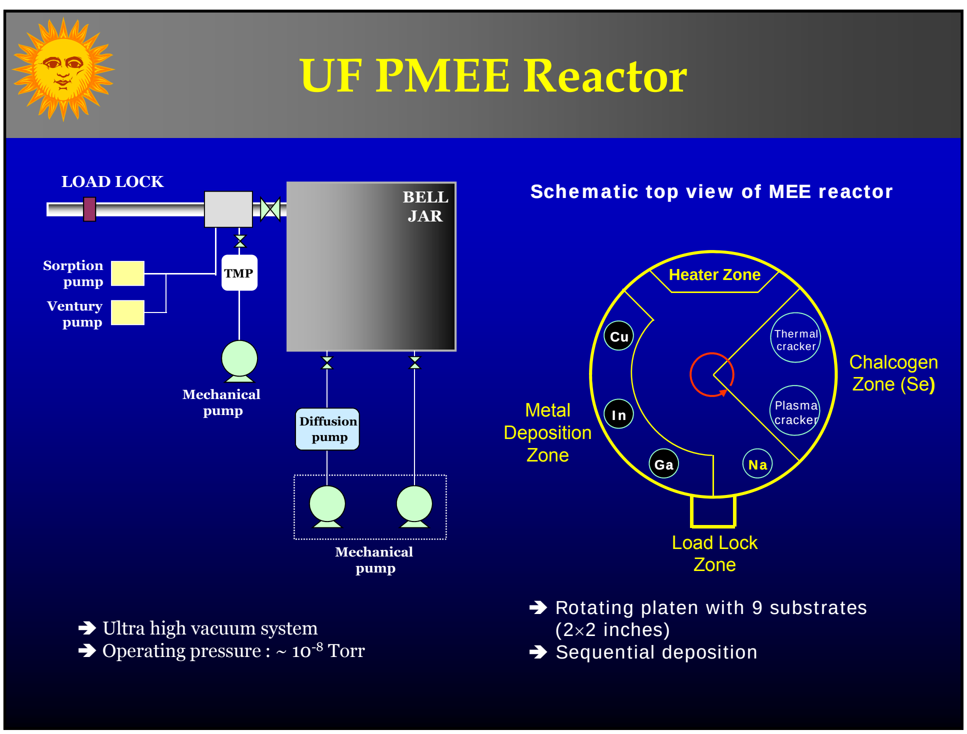
UF PMEE Reactor
LOAD LOCK
BELL JAR
Sorption pump
Ventury pump
TMP
Mechanical pump
Diffusion pump
Mechanical pump
➔ Ultra high vacuum system
➔ Operating pressure : ~ 10-8 Torr
Schematic top view of MEE reactor
Heater Zone
Thermal cracker
Plasma cracker
Chalcogen Zone (Se)
Cu
In
Ga
Na
Metal Deposition Zone
Load Lock Zone
➔ Rotating platen with 9 substrates (2×2 inches)
➔ Sequential deposition

Glass / Mo / γ-In_2Se_3 / Cu_2Se: RTXRD

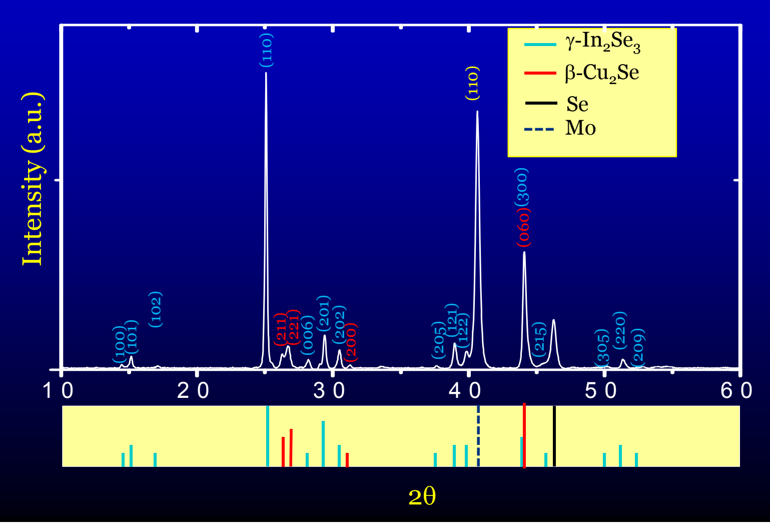

Glass/Mo/γ-In_2Se_3 /Cu_2Se/Se: Temperature Ramp Annealing

SS box Selenium Overpressure ~ 1 Torr

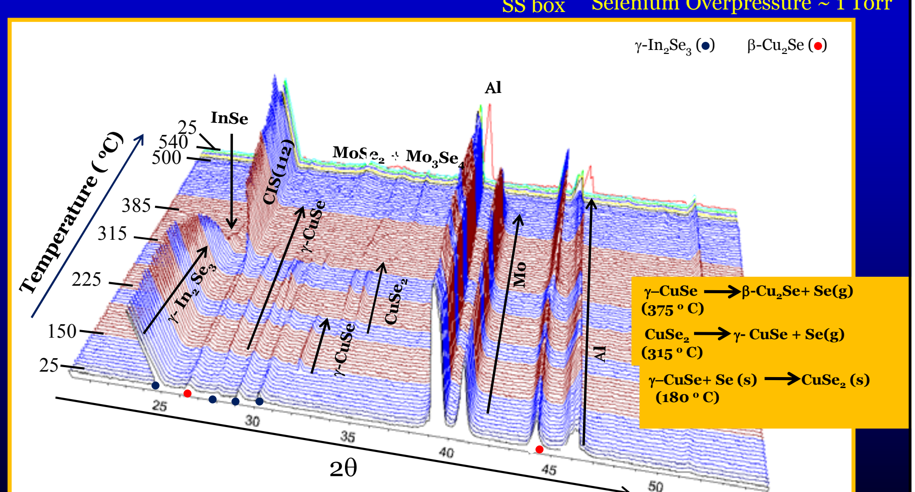

Cu-Se System Phase Equilibria

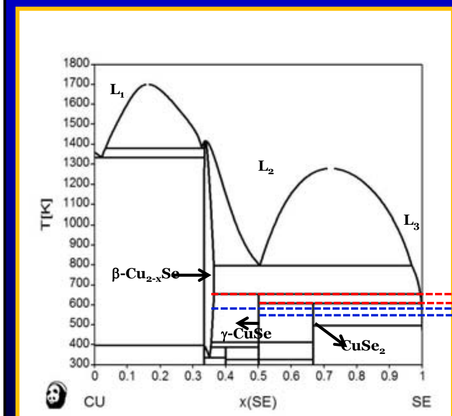

T-x Diagram

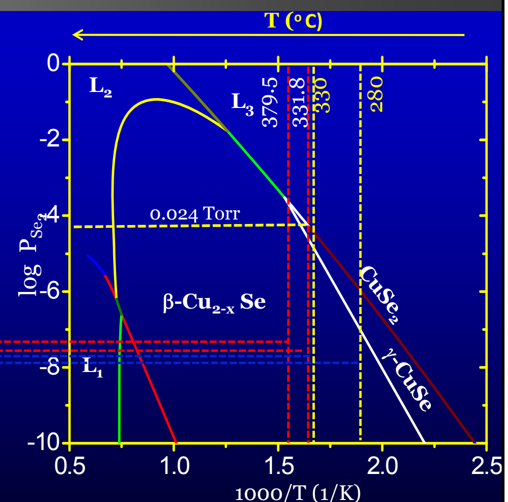

P-T Diagram

Glass/Mo/γ-In_2Se_3/Cu_2Se/Se: Temperature Ramp Annealing

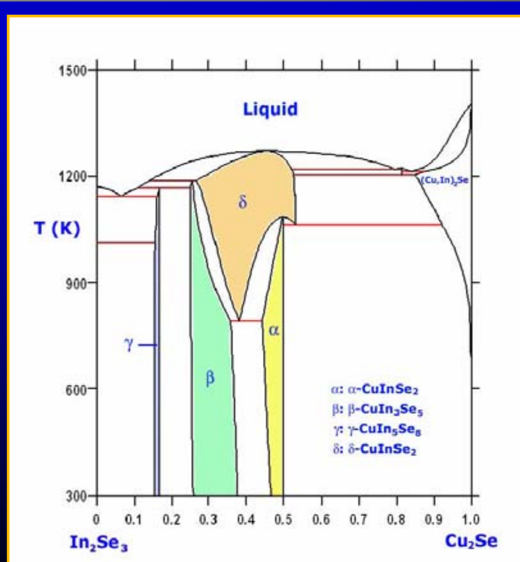

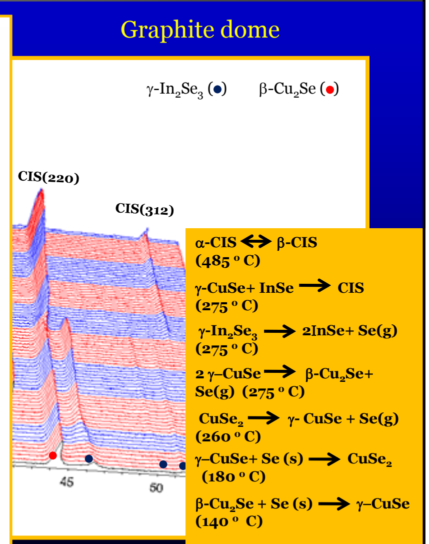

Isothermal Annealing
Glass/Mo/γ-In_2Se_3 /Cu_2Se/Se

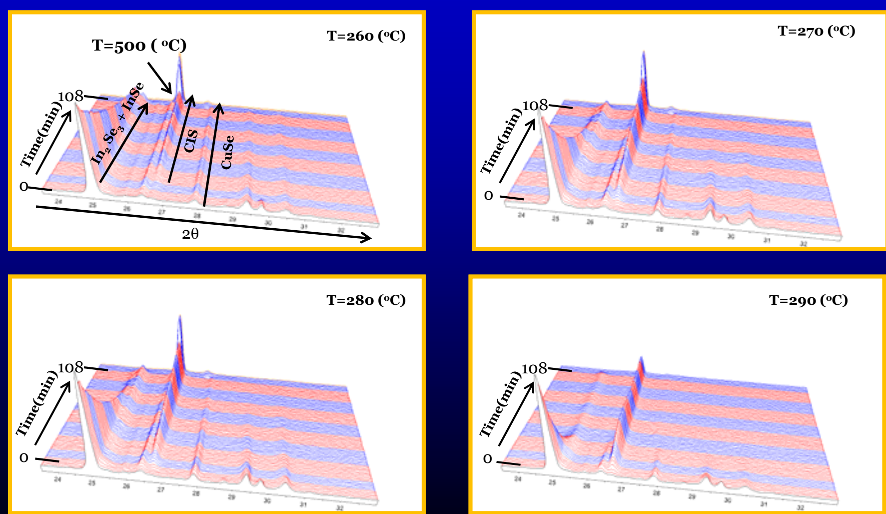

Solid-State Growth Models

- **Parabolic growth model**

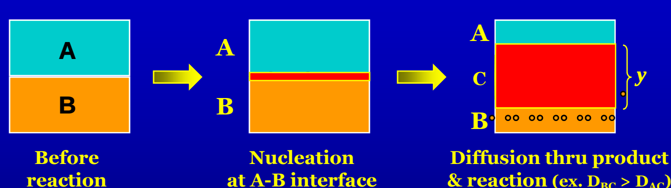

$$\frac{dy}{dt} = \frac{D \cdot k}{y}$$

$$y^2 = k_p \cdot t$$

- **Avrami growth model**

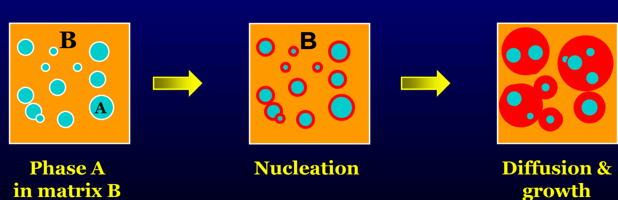

$$x = 1 - \exp[-(kt)^n]$$

$$\ln[-\ln(1-x)] = n\ln t + n\ln k$$

$0.5 < n < 1.5$
(1-D diffusion)

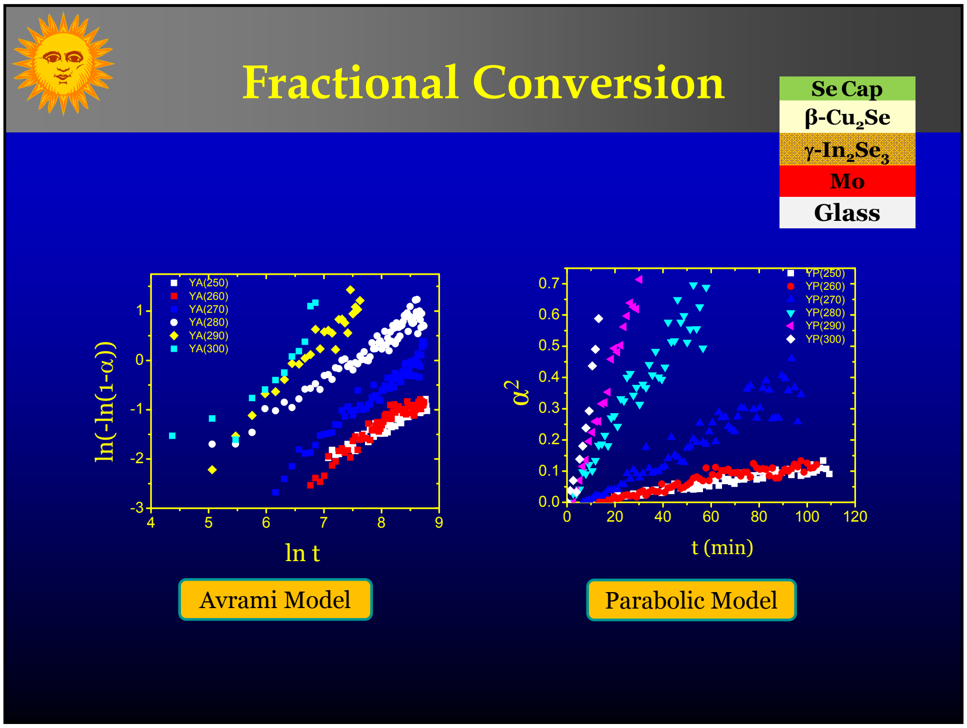
Fractional Conversion
Se Cap
β-Cu2Se
γ-In2Se3
Mo
Glass
ln(-ln(1-α))
ln t
YA(250)
YA(260)
YA(270)
YA(280)
YA(290)
YA(300)
α2
t (min)
YP(250)
YP(260)
YP(270)
YP(280)
YP(290)
YP(300)
Avrami Model
Parabolic Model

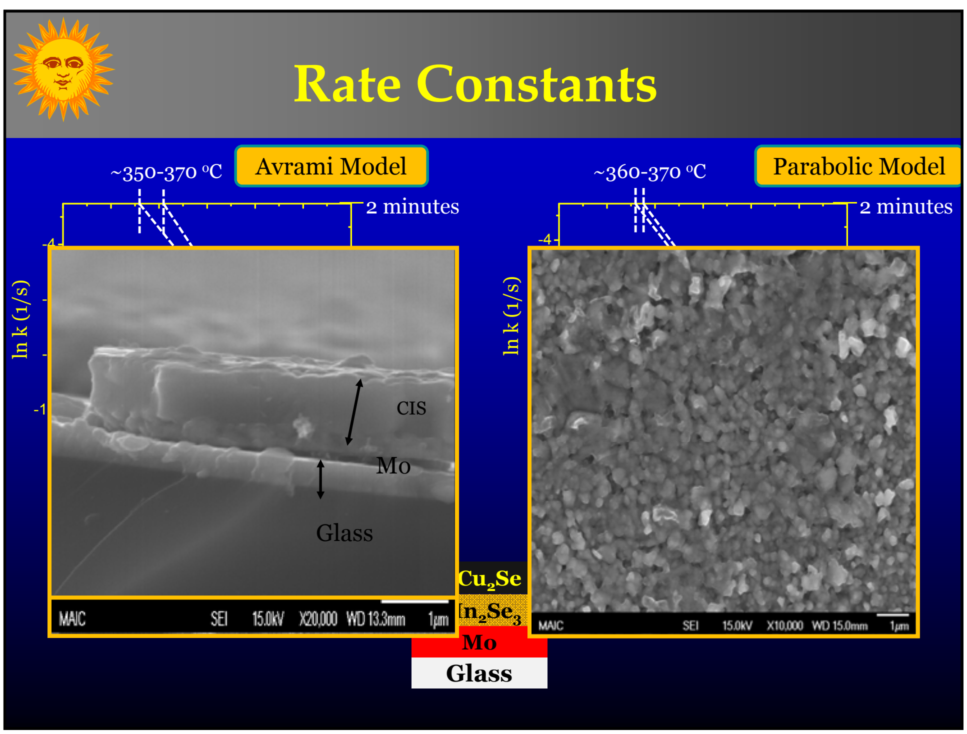
Rate Constants
~350-370 ºC
Avrami Model
2 minutes
ln k (1/s)
CIS
Mo
Glass
MAIC SEI 15.0kV X20,000 WD 13.3mm 1μm
~360-370 ºC
Parabolic Model
2 minutes
ln k (1/s)
MAIC SEI 15.0kV X10,000 WD 15.0mm 1μm
Cu2Se
In2Se3
Mo
Glass

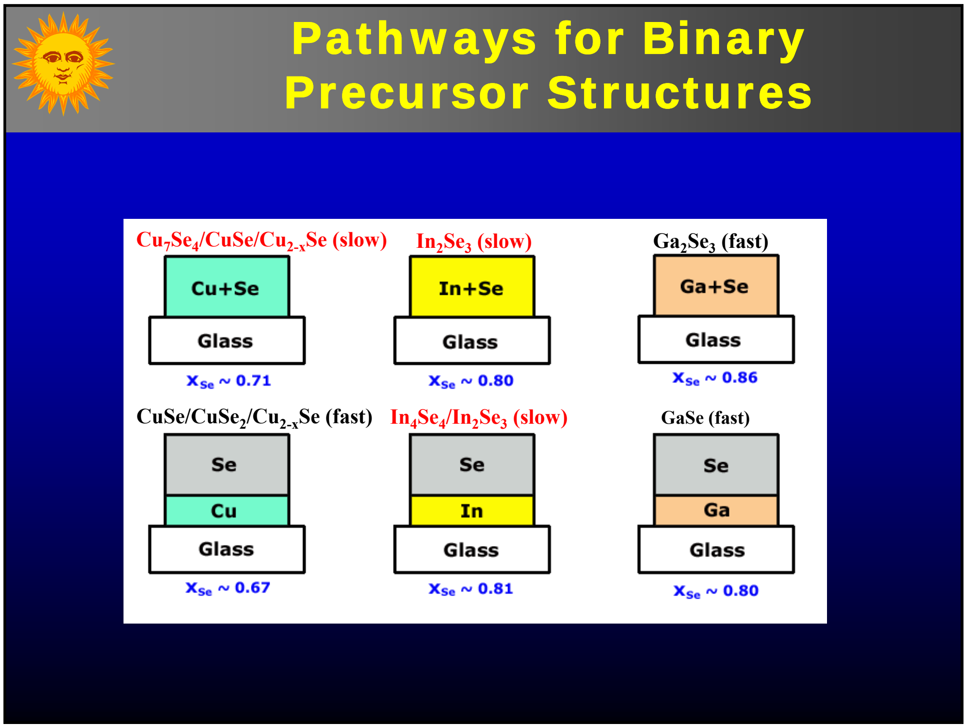
Pathways for Binary Precursor Structures
Cu_7Se_4/CuSe/Cu_{2-x}Se (slow)
Cu+Se
Glass
x_{Se} ~ 0.71
In_2Se_3 (slow)
In+Se
Glass
x_{Se} ~ 0.80
Ga_2Se_3 (fast)
Ga+Se
Glass
x_{Se} ~ 0.86
CuSe/$CuSe_2$/Cu_{2-x}Se (fast)
Se
Cu
Glass
x_{Se} ~ 0.67
In_4Se_4/In_2Se_3 (slow)
Se
In
Glass
x_{Se} ~ 0.81
GaSe (fast)
Se
Ga
Glass
x_{Se} ~ 0.80

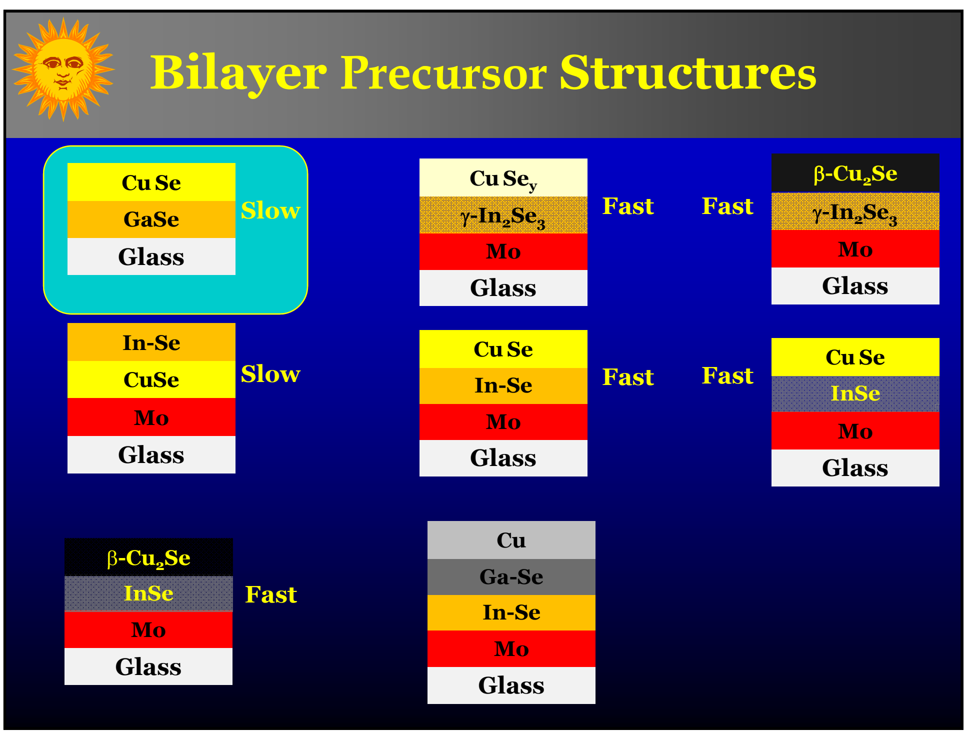
Bilayer Precursor Structures
Cu Se
GaSe
Glass
Slow
In-Se
CuSe
Mo
Glass
Slow
β-Cu_2Se
InSe
Mo
Glass
Fast
Cu Se_y
γ-In_2Se_3
Mo
Glass
Fast
Fast
β-Cu_2Se
γ-In_2Se_3
Mo
Glass
Cu Se
In-Se
Mo
Glass
Fast
Fast
Cu Se
InSe
Mo
Glass
Cu
Ga-Se
In-Se
Mo
Glass

Comparison of Interdiffusion in Various Intermetallics in Cu-In-Ga-Se

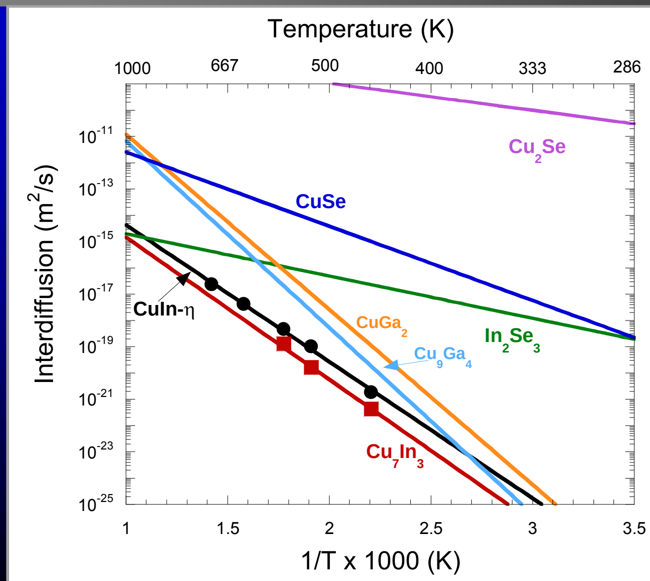

Metal Selenization Precursor Sets

Slow

- Se (1 μm)
- Ga (0.13 μm)
- In (0.216 μm)
- Cu (0.1 μm)
- Mo (0.6μm)
- SS

- Se (1 μm)
- Cu (0.1 μm)
- In (0.216 μm)
- Ga (0.13 μm)
- Mo (0.6μm)
- SS

Slow

Stacked Elemental Layer

- Ga (5 nm)
- In (70 nm)
- Cu(30 nm)

} 3 times

- Mo
- Glass

- Ga (2 nm)
- In (25 nm)
- Cu(10 nm)

} 6 times

- Mo
- Glass

*Modulated Structure

Glass/Mo/CuIn/CuGa: Temperature Ramp Annealing

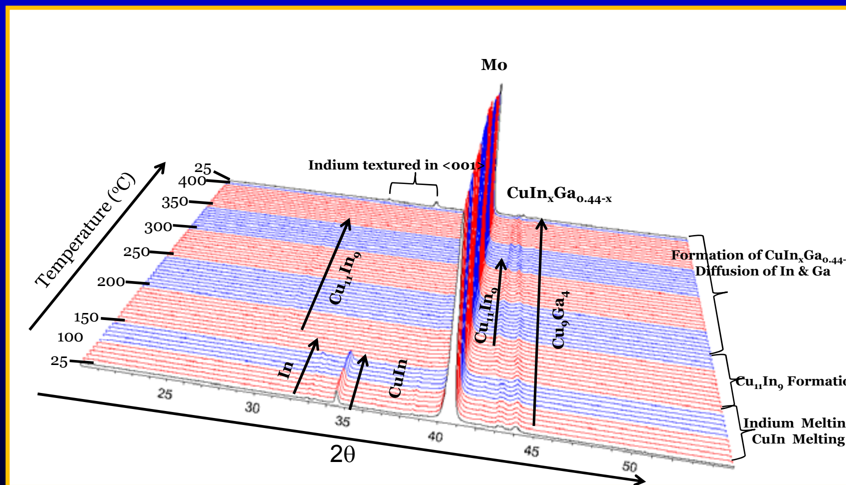

Cu-In-Ga Phase Diagram

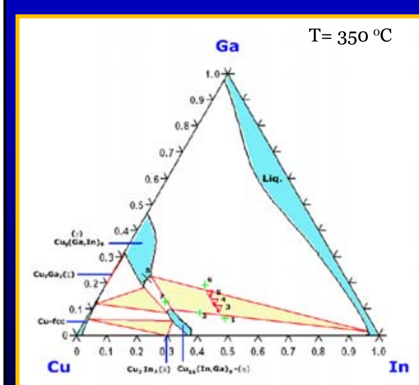

Phase Relationship at 350 ° C

No	Atomic Fraction			Equilibrium phases
	Cu	In	Ga	
1	0.479	0.458	0.063	$Cu_{16}(In,Ga)_9$, In
2	0.550	0.365	0.086	$Cu_{16}(In,Ga)_9$, In
3	0.479	0.417	0.104	$Cu_{16}(In,Ga)_9$, In, $Cu_9(In,Ga)_4$
4	0.479	0.391	0.130	$Cu_{16}(In,Ga)_9$, In, $Cu_9(In,Ga)_4$
5	0.479	0.359	0.161	$Cu_{16}(In,Ga)_9$, In, $Cu_9(In,Ga)_4$
6	0.479	0.328	0.193	In, $Cu_9(In,Ga)_4$
7	0.640	0.230	0.129	$Cu_{16}(In,Ga)_9$, $Cu_9(In,Ga)_4$
8	0.659	0.123	0.218	$Cu_9(In,Ga)_4$

Glass/Mo/CuIn/CuGa/Se: Temperature Ramp Annealing

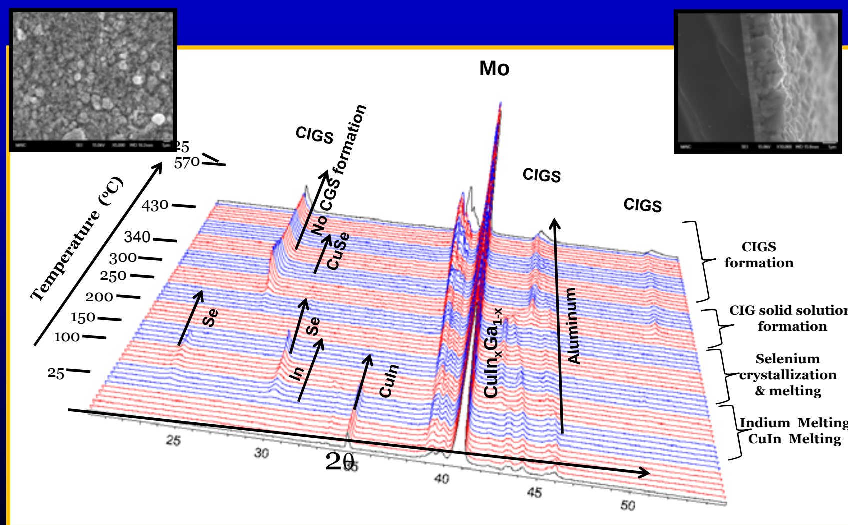

Temperature Ramp : Glass/Mo/CI/CG+ selenium vapor

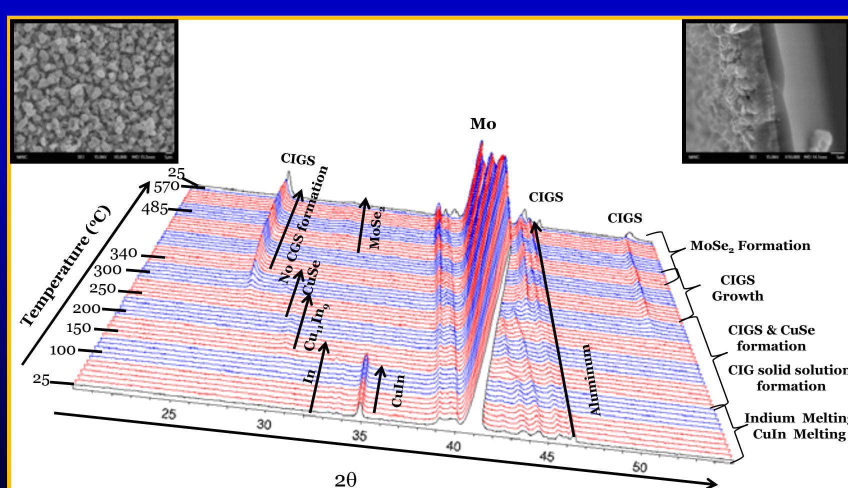

Ga Distribution

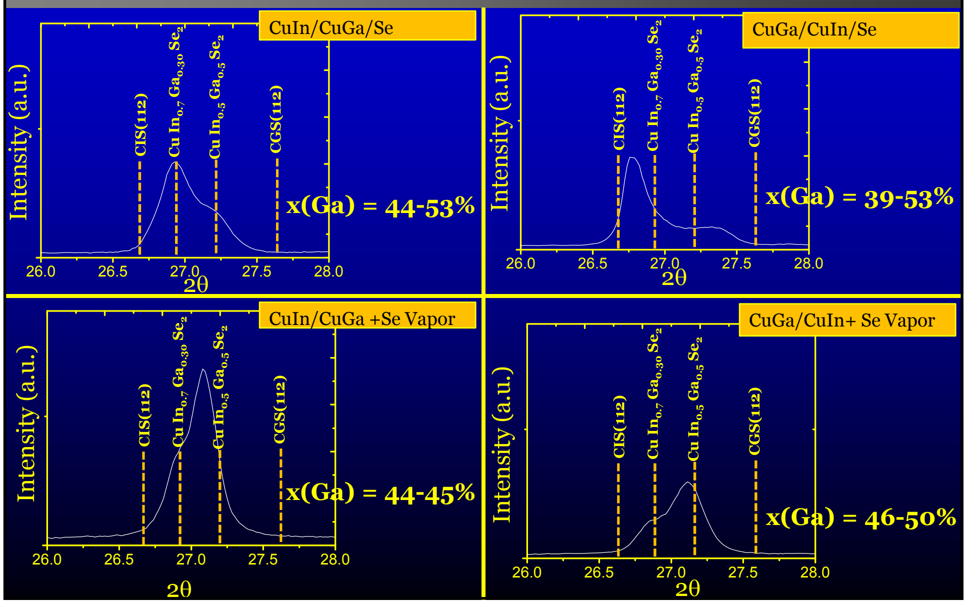

TEM-EDS

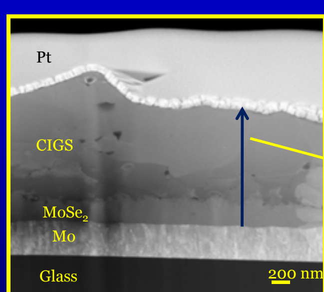

Dark Field Image

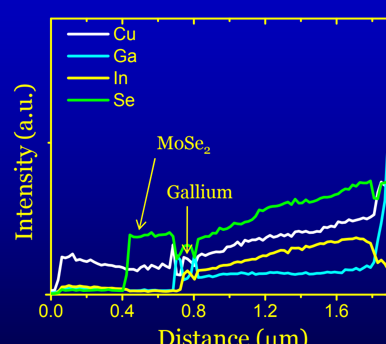

- ✓ $MoSe_2$ identified (300 nm) and same as previous sample (amorphous)
  Interface nature could not be determined
- ✓ Ga and In distributed non-uniformly across the thickness direction.
- ✓ More Ga towards the back contact.

Metal-Selenization Kinetics

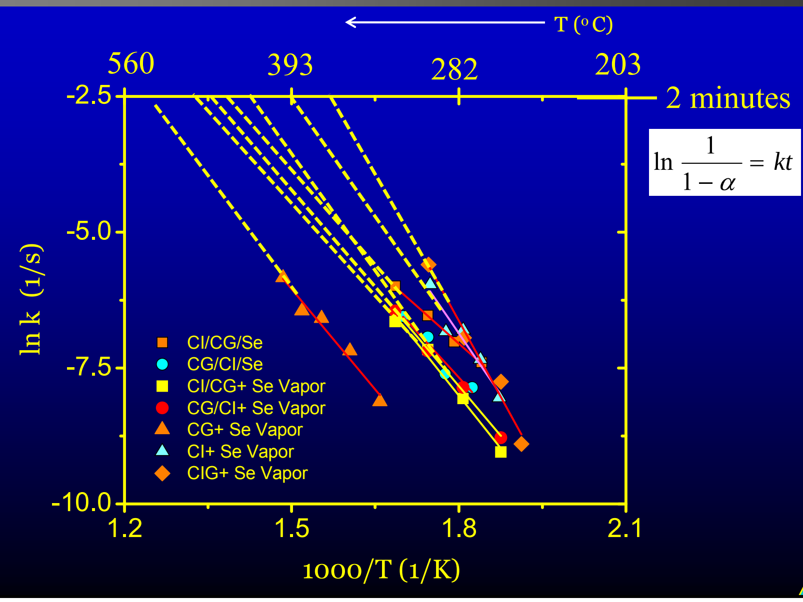

Role of $MoSe_2$ in CIGS

- **Literature suggests $MoSe_2$ - CIGS interfacial properties sensitive to processing conditions**
- **Modifies the contact resistance**
  - **Schottky contact without $MoSe_2$**
  - **Ohmic with but high resistance if $MoSe_2$ too thick or wrong orientation**
- **Influences adhesion characteristics**
  - **Poor adhesion without $MoSe_2$**
  - **Good adhesion depending on orientation**

Need better understanding of growth habit

o P.E. Russell et al., "Properties of the Mo-$CuInSe_2$ interface", *Appl. Phys. Lett.* **40**(11), 1984, pp. 995-997
o R.Wurz et al., "Formation of interfacial $MoSe_2$ layer in CVD grown $CuGaSe_2$ based thin film solar cells", *Thin solid films* **431-432**, 2003, pp.398-402

$MoSe_2$ Crystal Structure

- **Hexagonal Crystal Structure**
  - **Lattice constants:**

    a= 3.28 Å, c=12.9 Å
- **Strong Mo-Se covalent bonds in Se-Mo-Se layers**
- **Weak Van der Waals force between Se-Mo-Se layers**

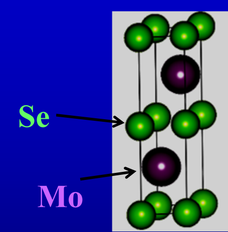

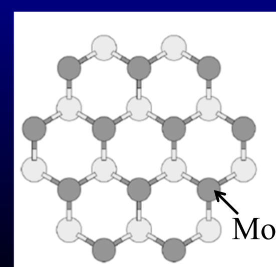

Temperature Ramp Selenization of Molybdenum in N_2/H_2 Atmosphere

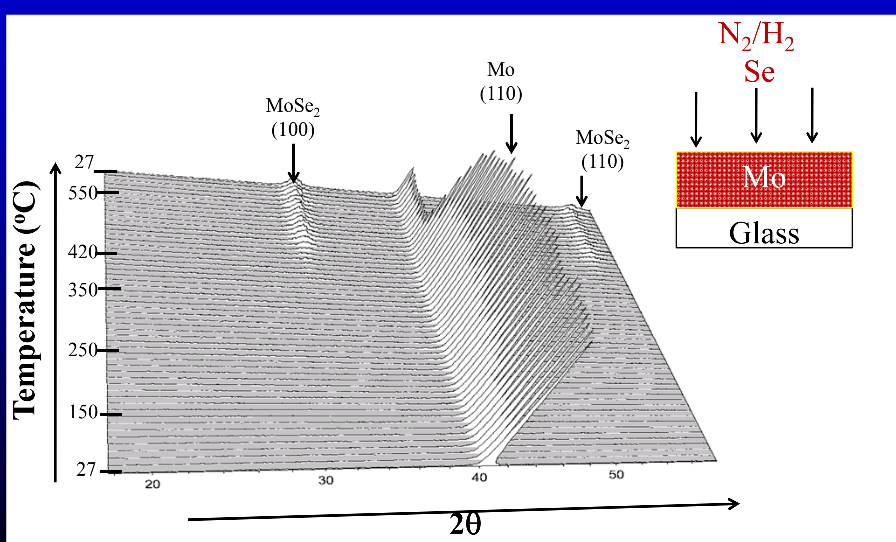

Kinetic Analysis

Avrami Model

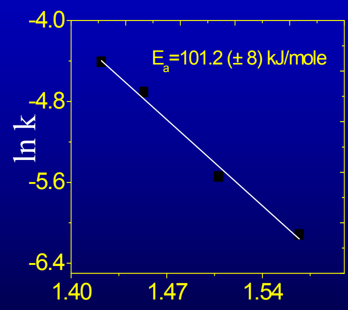

1000/T

Parabolic Model

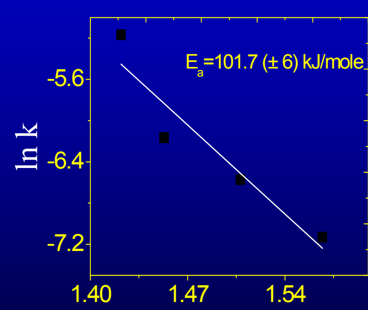

1000/T

$k=4.08\times10^5 \exp(-101.2/RT)$

$k=1.5\times10^5 \exp(-101.7/RT)$

Conclusions

- **Pathways are dependent on precursor structure**
  - **In phase particularly important**
- **Most paths are diffusion limited**
- **High-rate processes are possible**
  - **Film quality needs assessed**
  - **Liquid phase assisted growth**
- **Point defect chemistry helpful (low disordering energy)**
  - **Enhance diffusivity, defect compensation, type-inversion, impurity passivation**

Comparison between a Chemical Processing Plant and an Integrated Circuit

	TYPICAL CHEMICAL PLANT	*TYPICAL INTEGRATED CIRCUIT*
Raw material source	Many but depleting	Electrical ground
Number of species	10^2 or more	2 (electron, hole)
Transport	Pipe (10 inch O.D.)	Wire, metal interconnect (10^{-5} inch O.D.)
Storage	Tank (10^6 moles)	Capacitor (10^{-10} moles)
Pump	10 hp	10^{-9} hp (bipolar transistor)
Control	Gate valve	FET
	On-off valve	Transistor
	Check valve	Diode
Reactions	Many	Recombination/generation
Flow Rates	10^3 moles/s	10^{-11} moles/s
Unit operations	10^4/mi^2	10^{16}/mi^2
Cost	\$$10^8$ (\$$10^9$/mi^2)	\$$10^2$ (\$$10^9$/mi^2)
Diffusion coefficient	10^{-2} to 10^{-5} cm^2/s	10 to 10^3 cm^2/s
Reaction Rate	10^6 1/moles/s	10^{16} 1/moles/s